Progress In Electromagnetics Research, Vol. 142, 683–699, 2013

DC MAGNETIC CONCENTRATOR AND OMNI-DIRECTIONAL CASCADED CLOAK BY USING ONLY ONE OR TWO HOMOGENEOUS ANISOTROPIC MATERIALS OF POSITIVE PERMEABILITY

Fei Sun[1, 2] and Sailing He[1, 2, *]

[1]Department of Electromagnetic Engineering, JORCEP [Joint Research Center of Photonics of Zhejiang University and KTH], School of Electrical Engineering, Royal Institute of Technology (KTH), Stockholm S-100 44, Sweden

[2]Centre for Optical and Electromagnetic Research, Zhejiang Provincial Key Laboratory for Sensing Technologies, East Building #5, Zijingang Campus, Zhejiang University, Hangzhou 310058, China

Abstract—A novel concentrator for static magnetic field enhancement is proposed and designed utilizing transformation optics. Compared with other devices for static magnetic field enhancement, our device has many good features: first, our concentrator can achieve a DC magnetic field enhancement in a relatively large free space with high uniformity. Secondly, our concentrator is composed by only one or two homogenous anisotropic materials with principal value greater than zero (without any infinitely large or zero value), which can be achieved by using currently available materials. Thirdly, the geometrical shape of the proposed device determines the enhancement factor and the permeability of the device. After choosing suitable geometrical parameters, we can obtain a concentration with a suitable enhancement factor and a material requirement that is easily achievable. The proposed concentrator will have many important applications in many areas (e.g., magnetic resonance imaging and magnetic sensors). Based on the same theoretical model, we also proposed a cascaded shielding device cloak for static magnetic fields. The proposed DC magnetic shielding device can be realized without using any material of zero permeability, and will have potential applications in, e.g., hiding a metallic object from being detected by a metal locator.

Received 25 September 2013, Accepted 10 October 2013, Scheduled 10 October 2013
* Corresponding author: Sailing He (sailing@jorcep.org).

1. INTRODUCTION

Static or quasi-static magnetic fields play an essential role in many scientific areas and practical applications including magnetic resonance imaging (MRI) [1], wireless energy transmission [2], magnetic sensing (e.g., Hall sensors) [3], transcranial magnetic stimulation (TMS) [4], gene and drug delivery by magnetic nano-particles [5, 6], metal detection (e.g., mine detection), mass spectrometers, particle accelerators, etc.. Achieving a higher static magnetic field can be a big breakthrough in many areas. There are two ways to achieve higher static magnetic field: one way is using some active magnet, which has a drawback of extremely high power consumption [7]. The other way is using passive magnetic lenses or concentrators that can cause an external magnetic field to converge without consuming additional power [8–11]. Our attention is focused on designing passive DC magnetic concentrators in this paper.

Many different kinds of DC magnetic lenses or concentrators have been proposed. Some DC magnetic lenses are designed with ferromagnetic materials such as Ho, Dy, Fe, etc.. However, for a magnetic lens made of ferromagnetic materials, the enhancement is limited by the saturation magnetization [8]. To achieve a higher magnetic field enhancement, a superconductor with a high critical field H_c can be used. In recent years, many magnetic lenses based on superconductors have been designed and experimentally demonstrated [9–11]. However, magnetic lenses/concentrators based on purely superconductors have many disadvantages: refrigeration is required, the enhancement factor is very low, the region in which DC magnetic field is enhanced is very small, and the performance often degrades due to quenching and other factors.

Very recently, some DC magnetic lenses/concentrators have been designed based on transformation optics (TO) [12–14]. TO is a powerful theoretical tool that can be used to control the trace of electromagnetic waves and also the static electric or magnetic field. A DC magnetic energy harvesting device, which can create an enhanced static magnetic field of high uniformity in free space, has been designed by TO [12]. However, it still needs some anisotropic medium whose permeability is zero in one principle direction and infinite in the other principle direction. Based on the space folded transformation, we have designed a passive compact concentrator that can achieve an extremely high static magnetic field enhancement in a large free space region with high field uniformity, which may have potential applications in MRI [13]. However, some special materials with a negative DC permeability, which is still a topic under study, are needed for the realization. A DC magnetic field compressor based on finite embedded transformation has also been designed to achieve a high DC magnetic field with high gradient [14]. This novel magnetic compressor, which can be constructed with materials of positive permeability, will have potential applications in controlling magnetic nano-particles for gene and drug delivery. In the present paper, we design a DC magnetic concentrator based on space compression transformation. Compared with other devices which can also achieve DC magnetic field enhancement designed by TO, the present device has many advantages: first, our device can achieve a DC magnetic field enhancement in a relatively large free space region with relatively high uniformity by using currently available materials whose permeabilities are greater than zero. In quasi-static condition, our device can be realized by using ferromagnetic materials and meta-materials without superconductors. Therefore, our device does not need refrigeration (its performance will also not be influenced significantly by temperature) and does not have any quenching problem. Secondly, our device can be constructed with only one or two homogeneous anisotropic materials, and thus does not need complex gradient control. Thirdly, the DC magnetic field enhancement factor of our device can be tuned by adjusting some geometrical parameters of our device.

Besides DC magnetic enhancement, cloaking a DC or quasi-static magnetic field also has many applications (e.g., hiding a metallic object from being detected by a metal detector). A DC magnetic cloak based on the combination of ferromagnetic materials and superconductors has been proposed in 2012 [15]. However, the performance of this cloak is still limited by some required material whose permeability is ideally zero. Based on the same theoretical model for our DC magnetic concentrator, we also propose a DC magnetic cloak consisting of some cascaded shielding structures, which can be realized by using two homogenous anisotropic magnetic materials of positive permeability. Under a quasi-static condition, it can be accomplished through the combination of ferromagnetic materials and metamaterials without superconductors. Our device can be easily extended from DC to a low frequency band (e.g., 200 kHz for metal detection).

2. DESIGN METHOD

2.1. The DC Magnetic Concentrator

TO can establish a corresponding relationship between two spaces by using coordinate transformation [16, 17]. One space is a visual space (referred as the reference space) and the other is the real space. By designing the coordinates of transformations or the geometry of the reference space, one can obtain a different distribution of special materials in the real space, which can allow for many pre-designed functions (e.g., invisibility, optical illusions, subwavelength focusing, and etc.). The basic idea in this paper is the space compression transformation, which has been used for optical energy concentration [18, 19]. For simplicity, we consider a two-dimensional (2D) structure in this paper. As shown in Fig. 1, different colors have been used to classify different regions (similar to the structure given in Fig. 1 of Ref. [19], where, however, energy concentration for an optical field, instead of DC magnetic field, was considered; a half-structure has also been used to cloak an object on a half-space [20]). In the reference space, all regions are free space whatever colors are used. In the real space we have different permeability materials in different colored regions. The red region in the reference space is compressed into the red region in the real space. In the red region of the real space, the DC magnetic field will be enhanced. The green regions and yellow regions also have been correspondingly transformed from the reference space to the real space. In the white region (outside the green region), we choose an identical transformation, which means the white region in the real space is still free space. We divide the whole transformed region into many sub-triangles, and thus the transformation can be easily

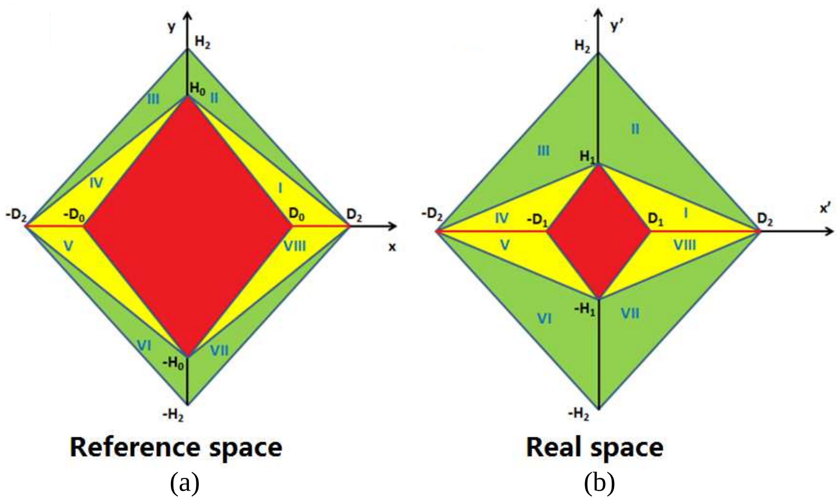

Figure 1. The transformation relations between the reference space and the real space. Red, yellow and green regions in each quadrant are correspondingly transformed from the reference space to the real space. White regions remain constant through the transformation.

determined by the corresponding relation of the vertices of triangles in the reference and real spaces. For ease of expression we number each sub-triangle region (e.g., I, II, III and etc. in Fig. 1). The reason why we divide the transformed regions into many sub-triangles is that once we use linear transformations to transform each sub-triangle, the corresponding permeability of transformed materials in the real space is constant in each sub-triangle region [20].

The corresponding materials in each region in the real space can be calculated using TO (see Appendix for details). The permeabilities in the yellow, green and red regions of the two-dimensional (2D) real space can be written respectively as:

$$\bar{\bar{\mu}}_{\text{yellow}}=\mu_0\begin{bmatrix}\frac{K_1}{K_3}+\frac{K_2^2}{K_1K_3} & \frac{K_2}{K_1}\\ \frac{K_2}{K_1} & \frac{K_3}{K_1}\end{bmatrix} \tag{1}$$

$$\mu_{\text{green}}=\mu_0\begin{bmatrix}\frac{1}{M_2} & \frac{M_1}{M_2}\\ \frac{M_1}{M_2} & \frac{M_1^2+M_2^2}{M_2}\end{bmatrix} \tag{2}$$

$$\bar{\bar{\mu}}_{\text{red}}=\mu_0\,\text{diag}\left(\frac{N_1}{N_2},\frac{N_2}{N_1}\right) \tag{3}$$

where

$$K_1=\frac{D_2-D_1}{D_2-D_0};\quad K_2=-\text{sign}(x')\text{sign}(y')\frac{D_2}{H_0}\frac{D_1-D_0}{D_2-D_0};\quad K_3=\frac{H_1}{H_0} \tag{4}$$

$$M_1=-\text{sign}(x')\text{sign}(y')\frac{H_1-H_0}{H_2-H_0}\frac{H_2}{D_2};\quad M_2=\frac{H_2-H_1}{H_2-H_0} \tag{5}$$

$$N_1=\frac{D_1}{D_0};\quad N_2=\frac{H_1}{H_0} \tag{6}$$

In order to make the DC magnetic field-enhanced region (red region) to be a free space and the whole structure to be more symmetric, we choose the following geometrical parameters:

$$\begin{aligned}D_1&=H_1=\alpha D_0=\alpha H_0\\ D_2&=H_2=\beta D_0=\beta H_0\end{aligned} \tag{7}$$

In order to achieve an effect of DC magnetic field concentration, α and β should satisfy that $0<\alpha<1$ and $\beta>1$. Substituting Eq. (7) into Eqs. (1)–(3), we obtain:

$$\bar{\bar{\mu}}_{\text{yellow}}=\mu_0\begin{bmatrix}\frac{(\beta-\alpha)^2+\beta^2(\alpha-1)^2}{\alpha(\beta-1)(\beta-\alpha)} & -\text{sign}(x')\text{sign}(y')\beta\frac{\alpha-1}{\beta-\alpha}\\ -\text{sign}(x')\text{sign}(y')\beta\frac{\alpha-1}{\beta-\alpha} & \frac{\beta-1}{\beta-\alpha}\alpha\end{bmatrix} \tag{8}$$

$$\bar{\bar{\mu}}_{\text{green}} = \mu_0 \begin{bmatrix} \frac{\beta-1}{\beta-\alpha} & -\text{sign}(x')\text{sign}(y')\frac{\alpha-1}{\beta-\alpha} \\ -\text{sign}(x')\text{sign}(y')\frac{\alpha-1}{\beta-\alpha} & \frac{(\alpha-1)^2+(\beta-\alpha)^2}{(\beta-1)(\beta-\alpha)} \end{bmatrix} \tag{9}$$

$$\bar{\bar{\mu}}_{\text{red}} = \mu_0 \text{diag}(1, 1) \tag{10}$$

In this case, the field-enhanced region (red region) is free space. As we can see from Eqs. (8)–(10), the required medium in each region is a homogenous anisotropic medium. Due to the symmetry of the transformed medium in the x'-y' coordinate system, the permeability tensor becomes diagonal in ξ-χ coordinate system (principal axis system):

$$\begin{bmatrix} \mu_{x'x'} & \mu_{x'y'} \\ \mu_{x'y'} & \mu_{y'y'} \end{bmatrix} \xrightarrow{\text{coordinate system rotates}} \text{diag}\left(\mu_{\xi\xi}, \mu_{\chi\chi}\right)$$

where

$$\begin{aligned} \mu_{\xi\xi} &= \cos^2\theta\mu_{x'x'} + \sin^2\theta\mu_{y'y'} + 2\sin\theta\cos\theta\mu_{x'y'} \\ \mu_{\chi\chi} &= \sin^2\theta\mu_{x'x'} + \cos^2\theta\mu_{y'y'} - 2\sin\theta\cos\theta\mu_{x'y'} \end{aligned} \tag{11}$$

and where

$$\theta = \frac{1}{2}\arctan\left(\frac{2\mu_{x'y'}}{\mu_{x'x'} - \mu_{y'y'}}\right) \tag{12}$$

Here θ (the principal axis angle) is the rotation angle between the x'-y' system and ξ-χ system (see the insert of Fig. 4(b)). Substituting Eqs. (8) and (9) into Eqs. (11) and (12) respectively, we can obtain the principal axis angle the permeability tensors in a diagonal form in the yellow and green regions.

Next we will use the finite element method (FEM) [21] to verify the performance of the device. We keep the size of the central red region (the DC magnetic field is enhanced in this region) $D_1 = 0.2\,\text{m}$ unchanged in the following simulations. Two key parameters α and β have been introduced during our design (see Eq. (7)). Let's first keep β constant and change α. As shown in Figs. 2(a)–(c), if β is unchanged, then as α decreases, the enhancement increases. This can be explained from the space compression. As the field in the red region with size D_0 in the reference space is compressed into the field in the red region with size $D_1 = \alpha D_0$ in the real space, the compression ratio of the space is α and the magnification ratio of the field is $1/\alpha$. In addition, we can also find that a smaller α corresponds to a larger size of the total device D_2 (deduced from Eq. (7)) and a higher degree of anisotropy of the medium (see Fig. 2(d)).

Next let us keep D_1 and α constant, while changing β. As shown in Figs. 3(a) to (c), if α remains the same, the enhancement factor in the red region is the same. From Eq. (7), we can also deduce that for

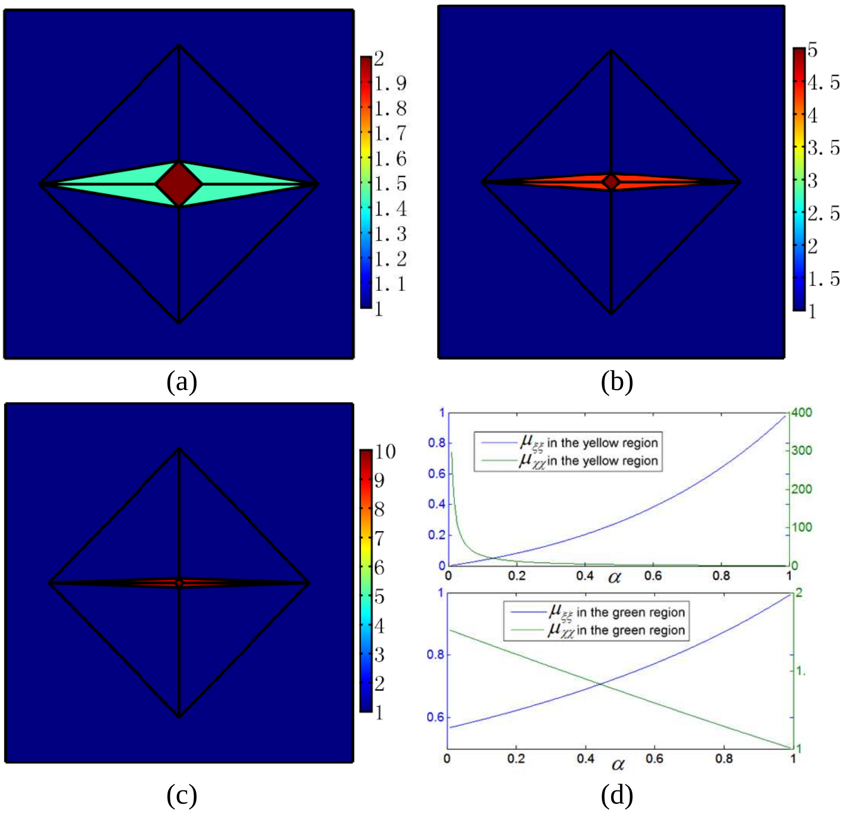

Figure 2. (a) to (c): FEM simulation results. We keep $D_1 = 0.2\,\mathrm{m}$ and $\beta = 3$ unchanged in each structure. Our concentration is surrounded by a uniform background DC magnetic field of amplitude 1 T (directed from top to bottom). The absolute value of the total DC magnetic flux density distribution when (a) $\alpha = 0.5$, (b) $\alpha = 0.2$, and (c) $\alpha = 0.1$. (d) The principal values [calculated with Eqs. (8), (9), (11) and (12)] of the permeability tensors of our concentration in the yellow and green regions when α changes from 0 to 1.

fixed D_1 and α, an increase in β results in a larger total size of the whole device D_2. From Fig. 3(d), it is apparent that an increasing β results in a smaller degree of anisotropy in all regions and the two principle values approaching to 1 in the green region (this can also be seen from the fact that the DC magnetic field in the green region is almost the same with the background DC magnetic field). Taking the

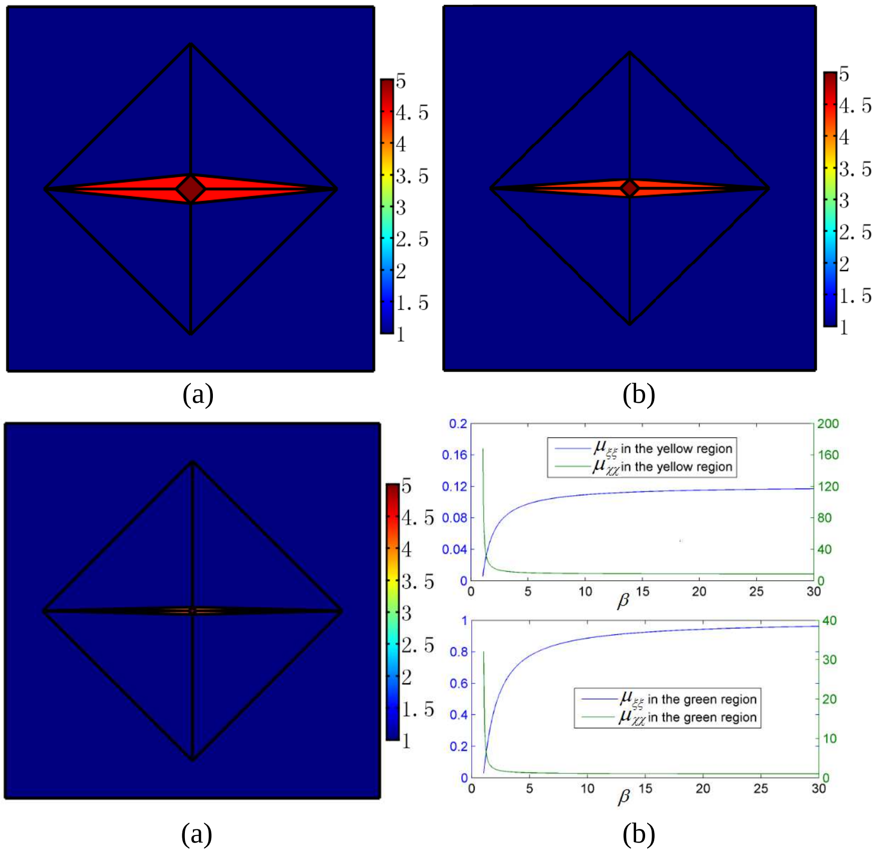

Figure 3. (a) to (c): FEM simulation results. We keep $D_1 = 0.2\,\text{m}$ and $\alpha = 0.2$ unchanged in each structure. When a uniform background DC magnetic field with amplitude 1T from top to bottom imposes onto our device, the absolute value of the total DC magnetic flux density distribution for (a) $\beta = 2$, (b) $\beta = 3$, and (c) $\beta = 8$. (d) The principal values of permeability of our concentrator in the yellow and green regions when β changes from 1 to 30 for $D_1 = 0.2\,\text{m}$ and $\alpha = 0.2$ fixed, which are calculated by Eqs. (8), (9), (11) and (12).

limit $\beta \to \infty$ in Eqs. (8) and (9), we can obtain:

$$\bar{\bar{\mu}}_{\text{yellow},\beta\to\infty} = \mu_0 \begin{bmatrix} \dfrac{1+(\alpha-1)^2}{\alpha} & -\text{sign}(x')\text{sign}(y')\,(\alpha-1) \\ -\text{sign}(x')\text{sign}(y')\,(\alpha-1) & \alpha \end{bmatrix} \tag{13}$$

$$\bar{\bar{\mu}}_{\text{green},\beta\to\infty} = \mu_0\,\text{diag}(1,1) \tag{14}$$

This explains why when β approaches to infinity, the medium in the green region in Fig. 1(b) will approach to free space. We can use this feature to further reduce the material requirement to realize such a DC magnetic concentrator. Our finial proposed DC concentrator is shown in Fig. 4(a), where we only need one homogenous anisotropic magnetic material to realize it and get about a 2.36 field enhancement factor in the center air region. In this case ($\alpha = 0.4$, $\beta = 10^5$ and $D_1 = 0.2\,\mathrm{m}$), the materials in the green region can approximately be treated as air (see Eq. (14)) and the shape of the yellow region can be approximately treated as a rectangle with two infinitely long sides parallel to the x' axis, which means that we can only use one anisotropic medium with two principal values of the permeability tensor greater than zero (see Eq. (13)) to realize a DC magnetic field concentration in a relative large free space region ($D_1 = 0.2\,\mathrm{m}$). The slight reduction of the performance in Fig. 4(a) is due to that when $\beta \to \infty$, the device is required to be infinitely long in the x' direction. However, we have to use a device with a finite size (2.8 m long in the x' direction) to make a simulation, and thus the enhancement degree of the device will be degraded.

To further pursue practical realization, next we will further study how to realize such a reduced concentrator with the same size ($D_1 = 0.2\,\mathrm{m}$) and same other parameters ($\alpha = 0.4$ and $\beta = 10^5$) of Fig. 4(a) by using a combination of ferromagnetic materials and diamagnetic materials. For the concentrator in Fig. 4(a), two principal values of the materials in the yellow region can be calculated using Eq. (13): $\mu_{\xi\xi} = 3.5155$ and $\mu_{\chi\chi} = 0.2845$. The principal axis angle can be determined using Eq. (11): $\theta = 10.9\,[\mathrm{deg}]$ in the first and third quadrants and $\theta = -10.9\,[\mathrm{deg}]$ in the second and fourth quadrants. Similarly, to build a DC magnetic half-space cloak [22], we can use two isotropic materials (μ_1 and μ_2) layer by layer to achieve an equivalent anisotropic medium in the yellow region. We choose duty-cycle 1 : 1 of two isotropic materials with permeability $0 < \mu_1 < 1$ and $\mu_2 > 1$. We choose two materials in parallel in the χ direction and in series in the ξ direction. By solving the following equations,

$$\begin{aligned} &\frac{\mu_1\mu_2}{\mu_1+\mu_2} = 0.14225; \\ &\mu_1+\mu_2 = 7; \end{aligned} \tag{15}$$

we can obtain: $\mu_1 = 0.145$ and $\mu_2 = 6.854$. The performance of the concentrator composed of these two isotropic materials layer by layer has also been verified by FEM (see Fig. 4(b)). In practice, $\mu_2 = 6.854$ can be easily achieved by using ferromagnetic materials, and $\mu_1 = 0.145$ can be achieved by using DC meta-materials [23]. This design may give a very practical way to realize our concentrator.

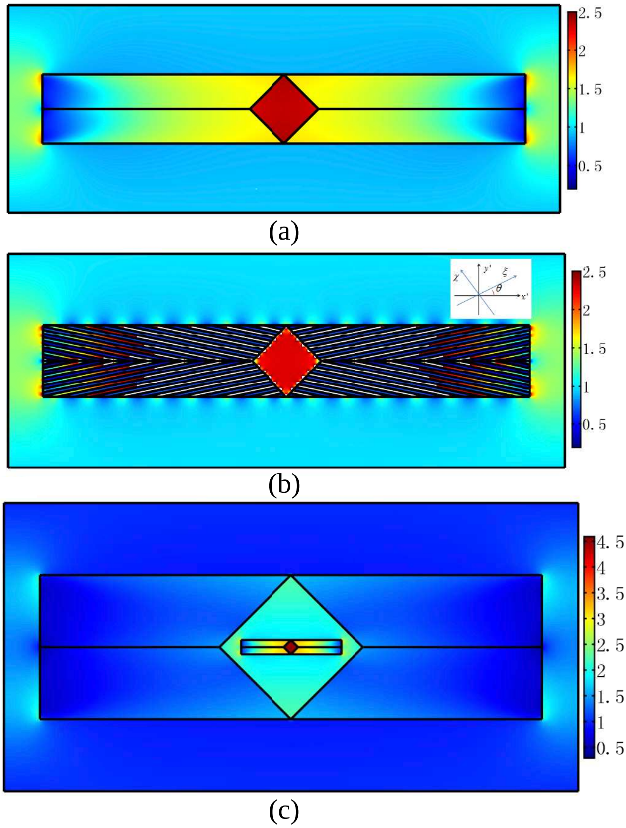

Figure 4. FEM simulation results for the absolute value of total magnetic flux density distribution, when a uniform background DC magnetic field (directed from up to bottom) of amplitude 1 T is imposed onto our proposed devices. (a) For a single concentrator with $D_1 = 0.2\,\mathrm{m}$ $\alpha = 0.4$ and $\beta = 10^5$. As β is extremely large in this case, we just drop the green region (the green region is air, see Eq. (14)) and only use a single yellow region to achieve this device. The permeability of the device (yellow region) is calculated with Eq. (8). (b) For a single concentrator composed of two isotropic materials $\mu_1 = 0.145$ and $\mu_2 = 6.854$ layer by layer. The geometrical parameters of this device are the same as the one in Fig. 4(a). The white region in Fig. 4(b) means that the magnetic field is larger than the largest value of the color bar. (c) For cascaded concentrators with $D_1 = 0.2\,\mathrm{m}$ and $D_1 = 2\,\mathrm{m}$ respectively. We still choose $\alpha = 0.2$ and $\beta = 10^5$ in both devices, and thus they are realized by only using the same material in the yellow region.

In some cases we have to choose a small α, which means small enhancement, to make the concentrator easily achievable in practice. Then we can use a cascaded concentrator to achieve a high DC magnetic field enhancement. As shown in Fig. 4(c), we use two concentrators both with $\alpha = 0.4$ and $\beta = 10^5$ to achieve an additional field enhancement compared with the single device in Fig. 4(a). Note that the two concentrators used in Fig. 4(c) have the same permeability as the device in Fig. 4(a) since the permeability is completely decided by α and β.

2.2. Cascaded Cloak for DC Magnetic Field

We can also design a DC magnetic cloak based on the above theoretical model (the same transformation relation explained in Fig. 1). As we can see from Fig. 1, if D_0 approaches to zero, the red region in the reference space will reduce to a single point. The red region in the real space corresponds to a single point in the reference space, and thus it will be totally invisible to the outside DC magnetic field. In this case both α and β approach to infinity (see Eq. (7)). However $\beta/\alpha = D_2/D_1$ is a finite value determined by the specific size of the device. FEM simulation verifies this idea, which is shown in Fig. 5(a). We should note that if both α and β approach to infinity, we can obtain an ideal DC magnetic cloak, which means no DC magnetic field can penetrate into the red region of the device. However, the two principal values of permeability in the yellow region of the cloak will approach to zero (this means it needs ideal superconductors) and infinity respectively. This would miss the advantage of our cloak compared with other recent DC magnetic cloak by using a combination of soft ferromagnetic materials and superconductors [15].

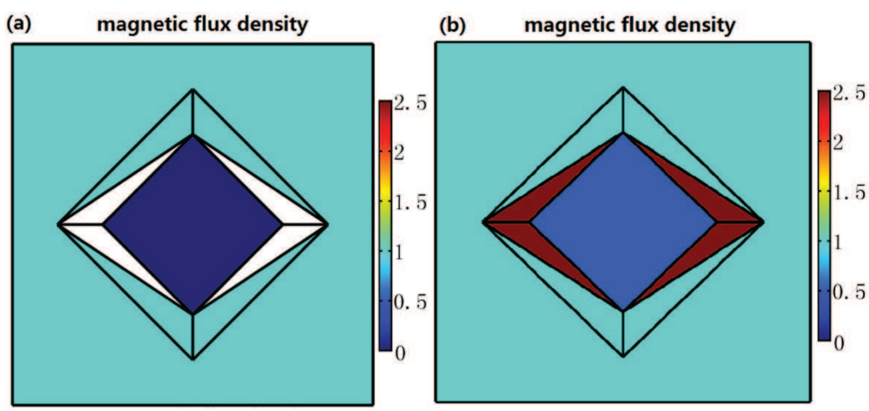

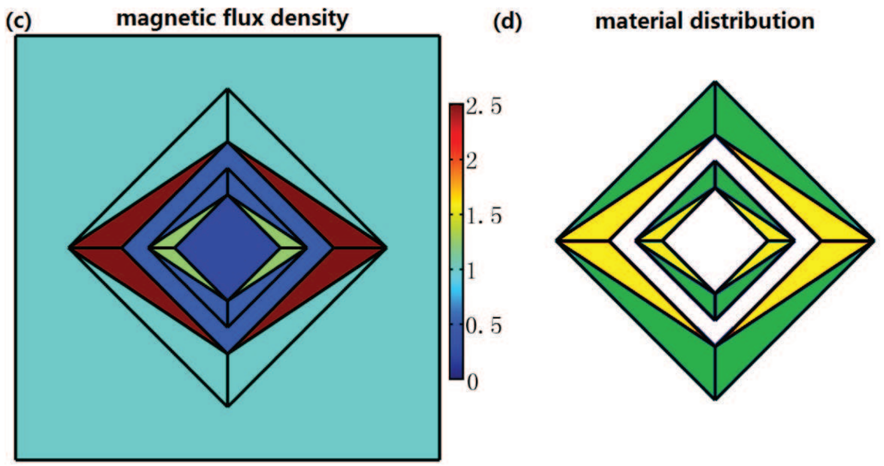

Figure 5. FEM simulation results for the absolute value of total DC magnetic flux density distributions when a uniform background DC magnetic field (directed from top to bottom) of amplitude 1 T is imposed onto our cloak. (a) We choose $D_1 = 2\,\mathrm{m}$, $D_2 = 3\,\mathrm{m}$, $\alpha = 2\times10^5$ and $\beta = 3\times10^5$ to construct a nearly ideal cloak for the DC magnetic field. In this case, the amplitude of the DC magnetic field in the cloaked region is 5×10^{-6} T (almost zero). (b) We choose $D_1 = 2\,\mathrm{m}$, $D_2 = 3\,\mathrm{m}$, $\alpha = 2$ and $\beta = 3$ to construct a shielding structure for DC magnetic field. In this case, the amplitude of the DC magnetic field in the center region is 0.5 T, which has been reduced by 50% from the external field. (c) Our proposed cascaded DC magnetic cloak consisting of two DC magnetic shielding structures. The geometrical shape of each shielding structure is the same as the one shown in Fig. 1(b). The inner one is the same as Fig. 5(b): $D_1 = 2\,\mathrm{m}$, $D_2 = 3\,\mathrm{m}$, $\alpha = 2$ and $\beta = 3$. The outer one is a similar to the inner one with $D_1 = 4\,\mathrm{m}$, $D_2 = 6\,\mathrm{m}$, $\alpha = 2$ and $\beta = 3$. In this case the amplitude of the DC magnetic field in the center region is 0.25 T, which has been reduced by 75% from the external field. The white region means that the magnetic field is larger than the largest value of the color bar. (d) The material distribution in our proposed cascaded cloak in (c). The yellow region is filled with a homogenous anisotropic material with principle value of permeability $\mu_{\xi\xi} = 7.673$ and $\mu_{\chi\chi} = 0.158$ (the principal axis angle θ is 37.98 deg in I, III quadrants and -37.98 deg in II, IV quadrants). The green region is filled with a homogenous anisotropic material with principle value of permeability $\mu_{\xi\xi} = 2.618$ and $\mu_{\chi\chi} = 0.382$ (the principal axis angle θ is -31.72 deg in I, III quadrants and 31.72 deg in II, IV quadrants). The white regions are free space.

Based on our theoretical model, we can design a cascaded DC magnetic shielding device that is easier to produce (without requiring materials of zero permeability) and can be extended to quasi-static field cases. The geometrical shape of a single magnetic shielding structure is the same as the structure in Fig. 1(b). Our idea is that if we can choose a relatively large α and β (infinity is not required and $\beta/\alpha = D_2/D_1$ remains), we can still obtain a good DC magnetic shielding effect (not an ideal cloak). Fig. 5(b) shows a single DC magnetic shielding structure when a background DC magnetic field of 1 T imposes onto the device, causing the DC magnetic field in the center of the free space region of the device to be 0.5 T (reduced by 50%) and keeping the outside magnetic field undisturbed. The two principal values in the yellow region (note that the yellow and green regions here are the same as those shown in Fig. 1(b)) of this device are $\mu_{\xi\xi} = 7.673$ and $\mu_{\chi\chi} = 0.158$ and the two principal values in the green region of the device are $\mu_{\xi\xi} = 2.618$ and $\mu_{\chi\chi} = 0.382$, which can also be realized by the combination of ferromagnetic materials and DC meta-materials. We can use two such DC magnetic shielding devices together (with identical permeability as α and β are the same in these two structures) to further shield the DC magnetic field (e.g., reduced by 75%; see Fig. 5(c)). The more shielding structures we cascade the better cloaking effect we can achieve and the material of each shielding structure is relatively easy to realize. We can cascade these magnetic shielding structures to realize every good DC magnetic shielding effect without using any superconductors in quasi-static condition. In addition, such a cascaded DC magnetic shielding device can also be easily achieved in the low frequency band (e.g., $f = 200\,\mathrm{kHz}$ for metal detection), as meta-materials can easily give a permeability with $0 < \mu < 1$ in low frequency band. We should note that the cloak proposed in [24] is only for one specific direction. In the present paper, we propose an omni-directional cloak formed by cascaded shielding structures using two kinds of homogeneous anisotropic materials of positive permeability. All the shielding structures (of geometric similarity) have different sizes but are formed with the same two kinds of materials which are easy to realize.

3. SUMMARY

We have designed a DC magnetic concentrator that can be easily realized using ferromagnetic materials and currently available DC meta-materials. The enhancement factor of our concentrator is determined by the geometrical parameters (α and β) of the device. Based on our concentrator, we can achieve an enhanced DC magnetic field in a relatively large free space region with relatively high uniformity. A reduction method ($\beta \to \infty$) has also been proposed to further simplify the realization of the device. A practical structure composed of the combination of ferromagnetic materials and diamagnetic materials has been designed to verify the performance of our concentrator. A cascaded DC magnetic cloak has also be designed based on our theoretical model, which can be constructed with ferromagnetic materials and DC meta-materials without any superconductors in quasi-static condition. These devices will have many potential applications in DC magnetic field enhancement and shielding.

ACKNOWLEDGMENT

This work is partially supported by the National High Technology Research and Development Program (863 Program) of China (No. 2012AA030402), the National Natural Science Foundation of China (Nos. 61178062 and 60990322), the Program of Zhejiang Leading Team of Science and Technology Innovation, Swedish VR grant (# 621-2011-4620) and AOARD. Fei Sun thanks Prof. Yungui Ma for some discussions and the China Scholarship Council (CSC) for the support (No. 201206320083).

APPENDIX A.

1. Determine the permeability in different transformed regions:

As shown in Fig. 1, the transformation in the yellow regions I, IV, V and VIII can be given as:

$$\begin{cases} x' = K_1 x + K_2 y - \mathrm{sign}(x)\dfrac{D_1 - D_0}{D_2 - D_0} D_2 \\ y' = K_3 y \\ z' = z \end{cases} \tag{A1}$$

where

$$K_1 = \frac{D_2 - D_1}{D_2 - D_0}; \quad K_2 = -\mathrm{sign}(x')\mathrm{sign}(y')\frac{D_2}{H_0}\frac{D_1 - D_0}{D_2 - D_0}; \quad K_3 = \frac{H_1}{H_0} \tag{A2}$$

Here sign function is introduced to generalize the formula in different quadrants. Note that yellow, green and red regions in each quadrant are correspondingly transformed from the reference space to the real space, and thus we have:

$$\mathrm{sign}(x) = \mathrm{sign}(x') = \begin{cases} 1, & x' \in \text{I, IV quadrants} \\ -1, & x' \in \text{II, III quadrants} \end{cases}$$

$$\mathrm{sign}(y) = \mathrm{sign}(y') = \begin{cases} 1, & y' \in \text{I, II quadrants} \\ -1, & y' \in \text{III, IV quadrants} \end{cases}$$

The transformation in the green regions II, III, VI and VII can be given as:

$$\begin{cases} x' = x \\ y' = M_1 x + M_2 y + \mathrm{sign}(y') \dfrac{H_1 - H_0}{H_2 - H_0} H_2 \\ z' = z \end{cases} \tag{A3}$$

where

$$M_1 = -\mathrm{sign}(x')\mathrm{sign}(y') \frac{H_1 - H_0}{H_2 - H_0} \frac{H_2}{D_2}; \quad M_2 = \frac{H_2 - H_1}{H_2 - H_0} \tag{A4}$$

We can also divide the red region into four sub-triangle regions in four quadrants, so that the transformation in each red sub-triangle can be given as:

$$x' = \frac{D_1}{D_0} x; \quad y' = \frac{H_1}{H_0} y; \quad z' = z \tag{A5}$$

with

$$N_1 = \frac{D_1}{D_0}; \quad N_2 = \frac{H_1}{H_0} \tag{A6}$$

As the behavior of the static magnetic field is still governed by Maxwell's equations, we can use TO to determine the transformed materials according to the above transformation [13]:

$$\bar{\bar{\mu}} = \mu_0 \bar{\bar{A}} \bar{\bar{A}}^T / \det\left(\bar{\bar{A}}\right) \tag{A7}$$

$\bar{\bar{A}}$ is the Jacobean matrix of the corresponding transformation. Thus the materials in each region can be calculated as follows.

In the yellow regions I, IV, V and VIII:

$$\mu_{\text{yellow}} = \mu_0 \begin{bmatrix} \frac{K_1}{K_3} + \frac{K_2^2}{K_1 K_3} & \frac{K_2}{K_1} & 0 \\ \frac{K_2}{K_1} & \frac{K_3}{K_1} & 0 \\ 0 & 0 & \frac{1}{K_1 K_3} \end{bmatrix} \tag{A8}$$

In the green regions II, III, VI and VII:

$$\mu_{\text{green}} = \mu_0 \begin{bmatrix} \frac{1}{M_2} & \frac{M_1}{M_2} & 0 \\ \frac{M_1}{M_2} & \frac{M_1^2 + M_2^2}{M_2} & 0 \\ 0 & 0 & \frac{1}{M_2} \end{bmatrix} \tag{A9}$$

In the red regions:

$$\mu_{\text{red}} = \mu_0 \,\mathrm{diag}\left(\frac{N_1}{N_2}, \frac{N_2}{N_1}, \frac{1}{N_1 N_2}\right) \tag{A10}$$

We only consider the two-dimensional structure, thus Eqs. (A8), (A9) and (A10) can be reduced to Eqs. (1), (2) and (3) in the main article.

REFERENCES

1. Brown, M. A. and R. C. Semelka, *MRI: Basic Principles and Applications*, Wiley-Blackwell, 2010.
2. Kurs, A., A. Karalis, R. Moffatt, J. D. Joannopoulos, P. Fisher, and M. Soljacic, "Wireless power transfer via strongly coupled magnetic resonances," *Science*, Vol. 317, No. 5834, 83–86, 2007.
3. Ripka, P. and M. Janosek, "Advances in magnetic field sensors," *IEEE Sens. J.*, Vol. 10, No. 6, 1108–1116, 2010.
4. Kobayashi, M. and A. Pascual-Leone, "Transcranial magnetic stimulation in neurology," *The Lancet Neurology*, Vol. 2, No. 3, 145–156, 2003.
5. Dobson, J., "Magnetic micro- and nano-particle-based targeting for drug and gene delivery," *Nanomedicine*, Vol. 1, No. 1, 31–37, 2006.
6. Veiseh, O., J. W. Gunn, and M. Zhang, "Design and fabrication of magnetic nanoparticles for targeted drug delivery and imaging," *Advanced Drug Delivery Reviews*, Vol. 62, No. 3, 284–304, 2010.
7. National High Magnetic Field Laboratory, http://www.magnet.fsu.deu/usershub/scientificdivisions/dcfield/facilities.html.
8. Iwasa, Y., "Hybrid magnets: A magnet engineer's experience and a proposal for the next generation of hybrids," *Physica B*, Vol. 216, Nos. 3–4, 186–192, 1996.
9. Kiyoshi, T., S. Choi, S. Matsumoto, T. Asano, and D. Uglietti, "Magnetic flux concentrator using Gd-Ba-Cu-O bulk superconductors," *IEEE Transactions on Applied Superconductivity*, Vol. 19, No. 3, 2174–2177, 2009.
10. Zhang, Z. Y., S. Matsumoto, S. Choi, R. Teranishi, and T. Kiyoshi, "Comparison of different configurations of NbTimagnetic lenses," *Supercond. Sci. Technol.*, Vol. 24, No. 10, 105012, 2011.
11. Zhang, Z. Y., S. Choi, S. Matsumoto, R. Teranshi, G. Giunchi, A. F. Albisetti, and T. Kiyoshi, "Magnetic lenses using different MgB_2 bulk superconductors," *Supercond. Sci. Technol.*, Vol. 25, No. 2, 025009, 2012.
12. Navau, C., J. Prat-Camps, and A. Sanchez, "Magnetic energy harvesting and concentration at a distance by transformation optics," *Phys. Rev. Lett.*, Vol. 109, 263903, 2012.
13. Sun, F. and S. He, "Create a uniform static magnetic field over 50 T in a large free space region," *Progress In Electromagnetic Research*, Vol. 137, 149–157, 2013.

14. Sun, F. and S. He, "Static magnetic field concentration and enhancement using magnetic materials with positive permeability," *Progress In Electromagnetic Research*, Vol. 142, 579–590, 2013.
15. Gomory, F., M. Solovyov, J. Souc, and C. Navau, "Superconductor-ferromagnetic metamaterials for magnetic cloaking and concentration," *Supercond. Sci. Technol.*, Vol. 26, 074001, 2013.
16. Leonhardt, U. and T. G. Philbin, *Geometry and Light: Science of Invisibility*, Dover, 2010.
17. Pendry, J. B., D. Schuring and D. R. Smith, "Controlling electromagnetic fields," *Science*, Vol. 312, No. 5781, 1780–1782, 2006.
18. Rahm, M., D. Schurig, D. A. Roberts, S. A. Cummer, D. R. Smith, and J. B. Pendry, "Design of electromagnetic cloak and concentrators using form-invariant coordinate transformations of Maxwell's equations," *Photonics and Nanostructures-Fundamentals and Applications*, Vol. 6, 87–95, 2008.
19. Li, W., J. Guan and W. Wang, "Homogeneous-materials-constructed electromagnetic field concentrators with adjustable concentrating ratio," *J. Phys. D: Appl. Phys.*, Vol. 44, 125401, 2011.
20. Chen, X., Y. Luo, J. Zhang, K. Jiang J. B. Pendry, and S. Zhang, "Macroscopic invisibility cloaking of visible light," *Nature Communications*, Vol. 2, 176, 2011.
21. The Finite Element Simulation is Conducted by Using Commercial Software COMSOL Multiphysics, http://www.comsol.com.
22. Wang, R., Z. L. Mei, and T. J. Cui, "A carpet cloak for static magnetic field," *Appl. Phys. Lett.*, Vol. 102, 213501, 2013.
23. Magnus, F., B. Wood, J. Moore, K. Morrison, G. Perkins, J. Fyson, M. C. Wiltshire, D. Caplin, L. F. Cohen, and J. B. Pendry, "A D.C. magnetic metamaterial," *Nature Materials*, Vol. 7, 295–297, 2008.
24. Landy, N. and D. R. Smith, "A full-parameter unidirectional metamaterials cloak for microwaves," *Nature Materials*, Vol. 12, 25–28, 2013.